

# Linear Nanostructure Formation of Aldehydes by Self-Directed Growth on Hydrogen-Terminated Silicon(100)

Jason L. Pitters,<sup>†</sup> Iana Dogel,<sup>‡</sup> Gino A. DiLabio,<sup>\*,†</sup> and Robert A. Wolkow<sup>\*,†,‡</sup>

National Institute for Nanotechnology, National Research Council of Canada, W6-010 ECERF, 9107 116th Street, Edmonton, Alberta, Canada T6G 2V4, and Department of Physics, University of Alberta, Edmonton, Alberta, Canada T6G 2J1

Received: September 12, 2005; In Final Form: November 2, 2005

The self-directed growth of organic molecules on silicon surfaces allows for the rapid, parallel production of hybrid organic–silicon nanostructures. In this work, the formation of benzaldehyde- and acetaldehyde-derived nanostructures on hydrogen-terminated H–Si(100)-2×1 surface is studied by scanning tunneling microscopy in ultrahigh vacuum and by quantum mechanical methods. The reaction is a radical-mediated process that binds the aldehydes, through a strong Si–O covalent bond, to the surface. The aldehyde nanostructures are generally composed of double lines of molecules. Two mechanisms that lead to double line growth are elucidated.

## Introduction

Several years ago it was demonstrated that styrene is capable of undergoing a remarkable radical-mediated, self-directed growth reaction that results in the formation of styrene-derived linear nanostructures covalently bound to an otherwise hydrogen-terminated silicon surface.<sup>1,2</sup> These original experiments showed that ordered, hybrid organic–silicon nanostructure growth was initiated at rare dangling bond (DB) sites on the silicon surface. Growth was found to occur through a self-directed growth mechanism, by simply exposing the silicon to gas-phase styrene. The mechanism for the “self-directed” growth of molecules on hydrogen-terminated Si surfaces has been described elsewhere.<sup>1,3</sup> Briefly, an alkene reacts with a DB on the silicon surface with concomitant formation of a carbon-centered radical. The carbon radical then abstracts a hydrogen atom from a neighboring silicon surface site to create a new silicon dangling bond that can react further with another alkene. The propagation of these reactions leads to multiple, sequential additions to form ordered lines of molecules on the silicon surface. On the silicon(100) surface, these lines tend to be confined to one side of a dimer row. The limited degree of human intervention in the process suggests that an unlimited number of ordered nanostructures can be rapidly and efficiently constructed in parallel.

We continue working toward establishing complete control over the many aspects of the synthesis of organic–silicon hybrid nanoassemblies. Thus far we have shown that the *extent of growth* may be controlled through protection–deprotection chemistry, by use of molecules to cap the ends of growing lines. The caps at the ends of those lines we wish to continue growing can then be selectively removed.<sup>4,5</sup> Some control over the *direction of growth* can be established by using different reconstructions of the underlying silicon surface<sup>6</sup> or, potentially, through the use of molecules that undergo a post-attachment rearrangement, such as “radical clocks”.<sup>7</sup> It is also important to have control over the *composition* of the nanostructures so that diversity and functionality can be established, and it has already

been demonstrated that various alkenes will create diverse nanostructures on silicon surfaces.<sup>1,3–8</sup> However, with one exception,<sup>7</sup> only nanostructures based on alkene–silicon reactions have been reported, and other means of attachment of analogous nanostructures have not been explored.

In this work, we report the formation of nanostructures that are bound to the silicon(100) surface through an oxygen atom. The use of an oxygen atom linker in place of a carbon linker atom has advantages in that the oxygen–silicon bond is stronger than the carbon–silicon bond and may lead to nanostructures that have a higher stability. Aldehydes have been used to form monolayer and macroscopic patterns on silicon by wet chemical methods<sup>9,10</sup> but have not been explored for their potential to form nanostructures in the self-directed manner described above. Here, we use scanning tunneling microscopy (STM) to study the growth of linear nanostructures of benzaldehyde and acetaldehyde under ultrahigh vacuum (UHV) conditions. The line-growth energetics are also studied by density functional theory (DFT) and compound ab initio methods.

## Experimental and Computational Methods

STM measurements (Omicron VT AFM/STM) were performed at room temperature in an ultrahigh vacuum (UHV) chamber with a background pressure of  $5 \times 10^{-11}$  Torr. N-type (As, 5 mΩ·cm) Si(100) crystals were used in all experiments. Silicon crystals were degassed overnight at 600 °C prior to generation of a clean surface by flashing the crystal to 1250 °C. Hydrogen-terminated Si(100)-2×1 surface were formed by heating the clean surface to 330 °C during exposure to atomic hydrogen. Benzaldehyde and acetaldehyde were purchased from Aldrich and were subjected to several freeze–pump–thaw cycles prior to use. Exposures of the silicon surfaces to reactants were performed by dosing the molecules into the vacuum chamber through a variable leak valve while monitoring the uncorrected pressure gauge readings. Mass spectrometric analysis of the UHV chamber during the dosing confirmed the high purity of the dosed molecules.

All calculations were performed with the Gaussian 03 suite of programs.<sup>11</sup> Reactions were modeled on a two-dimer, Si<sub>15</sub>H<sub>19</sub> silicon cluster representing a hydrogen-terminated silicon(100)-

\* Authors to whom correspondence should be addressed: e-mail Gino.DiLabio@nrc.ca (G.A.D.), rwolkow@ualberta.ca (R.A.W.).

<sup>†</sup> NINT–NRC.

<sup>‡</sup> University of Alberta.

$2 \times 1$  surface with a single surface dangling bond. This cluster has three surface hydrogen atoms, and the remaining 16 H atoms cap the dangling silicon back-bonds. The positions of the capping hydrogen atoms were kept frozen for all of the calculations, except those performed to obtain vibration frequencies. Structures were optimized at the B3P86<sup>12,13</sup>/6-31G\* level of theory, and single-point energies were computed with B3P86/6-311G(2d,2p). This model approach has been shown to accurately predict substituent effects on bond dissociation enthalpies.<sup>14</sup> Zero-point energies were obtained from scaled frequencies (scale factor = 0.9806<sup>14</sup>) computed with B3P86/6-31G\* on structures wherein the positions of the capping hydrogen atoms were relaxed. Hydrogen atom transfer transition-state structures were optimized by incrementing the distance between the transferring H and the carbon centered radical by 0.05 Å while the positions of the noncapping H and the Si atoms were allowed to relax. Additional single-point energy calculations on smaller models of the full systems<sup>15</sup> were performed with B3P86/6-311G(2d,2p) and the G3MP2 method.<sup>16</sup> In the smaller models, the phenyl rings were replaced by a hydrogen atom and the cluster was pared down to four or five silicon atoms, depending on the reactions. This was done to make the G3MP2 calculations feasible. The energies computed at the different levels of theory were used to calculate reaction zero-point corrected energies and barrier heights in an ONIOM-type scheme.<sup>17</sup> Similar cluster-type calculations have been used to study the thermochemistry of line growth processes.<sup>3,6–8,18</sup> Others groups have studied line growth using planewave formalisms.<sup>19–21</sup> The different approaches tend to produce results that are in quantitative agreement. Our own efforts have shown that thermochemistry results are essentially converged with respect to cluster size with a two-dimer cluster.

## Results and Discussion

Figure 1 shows large-area STM images of a hydrogen-terminated Si(100) surface before and after exposure to benzaldehyde. The diagonal bars in Figure 1A represent rows of silicon dimers. The bright spots in the image are dangling bonds on the hydrogen-terminated silicon surface, that is, silicon atoms that have not been terminated by hydrogen. After exposure of the surface to benzaldehyde ( $2 \times 10^{-7}$  Torr for 25 s = 5 L), linear nanostructure growth occurred at the majority of dangling bonds. The extent of the reaction reflects the fact that the benzaldehyde line growth reaction is robust. Figure 1B shows that the majority of the nanostructures are composed of double lines; that is, benzaldehyde molecules have chemisorbed to each atom of the silicon dimers. In rare instances, single lines can be found in addition to structures of mixed phases of double and single lines. This reaction mode is different from alkene nanostructure formation, where styrene molecules,<sup>1,4,5</sup> for example, tend to grow along one side of a dimer row. It is possible for alkenes to grow double lines when growth occurs along one side of a dimer row and then in the reverse direction along the same row. However, alkene double line growth occurs with low frequency.

The two possible mechanisms for line growth are illustrated in Figure 2. Following the essentially barrier-free addition of the aldehyde to the surface DB ( $A \rightarrow C$ ), the subsequent hydrogen-atom abstraction can occur from a silicon on the next dimer in the row ( $C \rightarrow E$ ) or from the silicon on the same dimer ( $C \rightarrow G$ ). A single line is formed if the  $C \rightarrow E$  mechanism repeats. This is the case for alkenes. A double line can be formed from the single line if one  $C \rightarrow G$  reaction occurs, followed by multiple  $C \rightarrow E$  steps in the reverse direction on the same dimer row. This “antiparallel” mechanism for the formation of double

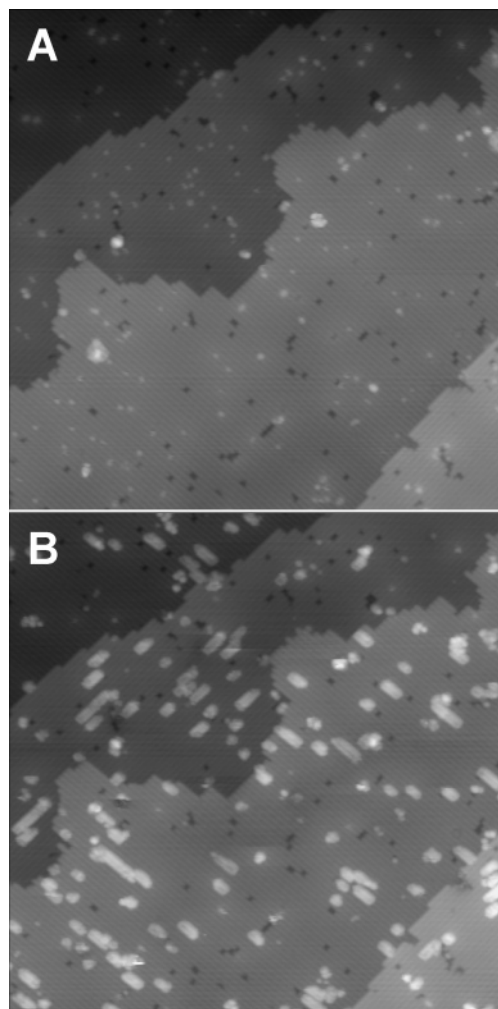


**Figure 1.** (A) STM image of unreacted hydrogen-terminated silicon. The small bright spots are dangling bonds on the surface. (B) STM of the same region after a 5 Langmuir dose of benzaldehyde. Virtually all dangling bonds have reacted with the benzaldehyde. Most of the lines appear as double lines. STM images:  $80 \times 80$  nm,  $-2.2$  V,  $0.063$  nA.

lines is illustrated in Figure 3A. Alternatively, if mechanism  $C \rightarrow G$  occurs initially, an aldehyde will add to the silicon on the same dimer. The ensuing hydrogen atom abstraction must occur from a silicon atom on the next dimer in the row. Therefore, alternating  $A \rightarrow E$  and  $A \rightarrow G$  reactions will lead to a double line through a “square wave” growth pattern, which is illustrated in Figure 3B. Both line-growth mechanisms result in molecular lines that are terminated with a silicon DB.

Figure 4 shows STM images that capture both the square wave and the antiparallel growth mechanisms in progress. In Figure 4A, a double line terminated by a DB is imaged. This double line may have formed initially through either mechanism. A subsequent dose of benzaldehyde results in an extension of the original double line that maintains a dangling bond at its end, see Figure 4B. Thus, the extended portion grew according to the square wave pattern. If the antiparallel mechanism had occurred, the dangling bond could not have been at the end of the line but instead would have been located in the interior of the line, surrounded by molecules. Figure 4C,D shows the antiparallel mechanism in progress. Figure 4C shows a nanostructure composed of double line and single line segments. The dangling bond is at the end of the single line segment, indicating that the double line portion was formed first, by either the antiparallel or square wave growth patterns or some combination

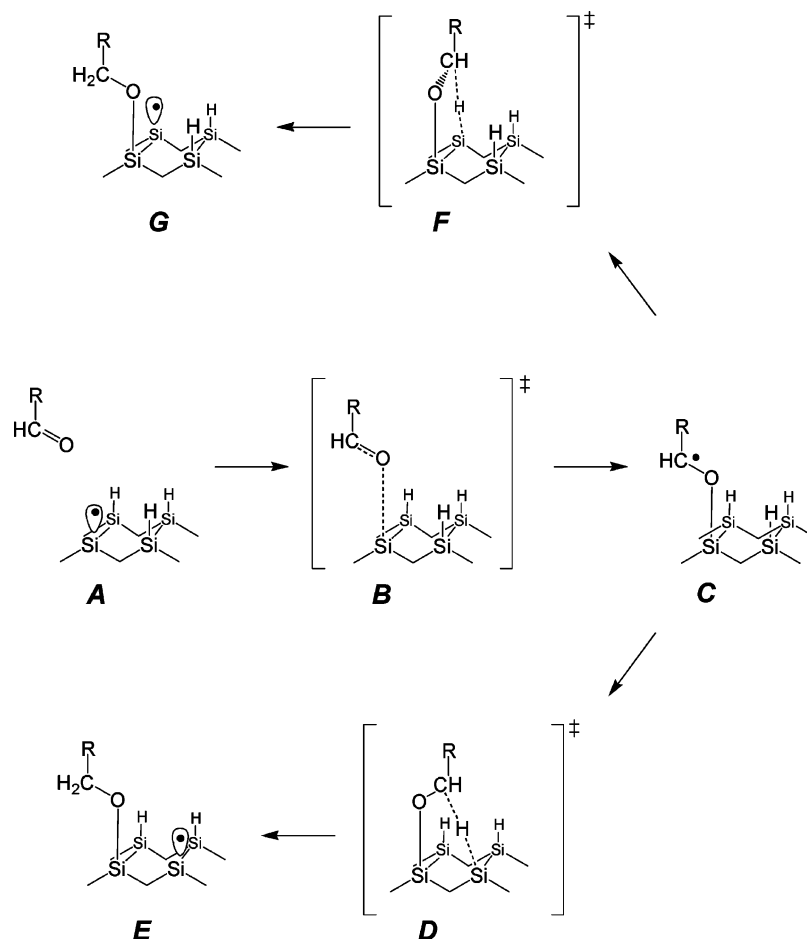


**Figure 2.** Reaction mechanisms for the self-directed growth of aldehyde lines on H-Si(100)-2×1. For benzaldehyde, R = C<sub>6</sub>H<sub>5</sub>, and for acetaldehyde, R = CH<sub>3</sub>. The calculated C---H distances in the transition-state structures are 1.65–1.70 Å.

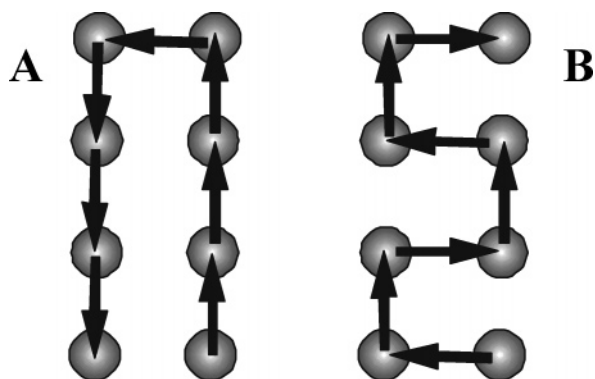


**Figure 3.** Cartoon representing (A) antiparallel and (B) square wave growth mechanisms for the formation of double lines. Horizontal pairs of circles represent a silicon dimer on the H-Si(100)-2×1 surface. The tail of the arrow indicates the adsorption site for the aldehyde, while the head of the arrow indicates the site of hydrogen abstraction.

of the two. Further exposure of the nanostructure to benzaldehyde creates a structure that has the DB surrounded by molecules, indicating that the new portion of the double line was formed by the antiparallel process.

Because there are two competing mechanisms for the growth of lines, it is inevitable that nanostructures with mixtures of single and double lines will be observed. Figure 4C provides an example of a double line that has grown into a single line. Figure 5A shows a nanostructure composed of a single line and a double line segment. Figure 5B shows multiple nanostructures, one of which has switched between double and single line growth several times.

The results of our theoretical calculations, given in Table 1, help us to understand the experimental observations. The addition of a C=O double bond containing species to a silicon dangling bond (A → C in Figure 2) typically proceeds with a small barrier (ca. 0.1 eV).<sup>22</sup> Benzaldehyde binds to the surface and releases 1.4 eV of energy. This large exoergicity is due to the strong Si–O  $\sigma$ -bond that is formed upon addition and to the stability gained through the delocalization of the unpaired electron on the carbon-centered radical into the aromatic ring.<sup>23</sup> Hydrogen abstraction from a silicon on the next dimer (C → D) results in growth along a dimer row (parallel/antiparallel growth) and has a barrier height of 1.0 eV. This barrier is 0.4 eV lower than the benzaldehyde addition energy. The hydrogen abstraction from the next dimer is effectively thermoneutral, but overall the addition/abstraction process is exoergic by 1.4 eV. The abstraction of the hydrogen atom on the same dimer (C → G) has the same exoergicity as the next dimer abstraction but is calculated to have a barrier (C → F) of 0.9 eV; that is, essentially equal to the barrier associated with parallel/antiparallel growth.<sup>24</sup> This explains the mixture of nanostructures grown via the parallel/antiparallel and square wave growth patterns.

The barriers to the hydrogen atom abstractions are consistent with those computed in previous work.<sup>18,19b,20,21</sup> These barriers are lower than that associated with molecular desorption, which supports the proposed reaction mechanism. The rates of abstraction are calculated by classical transition-state theory to be between 10<sup>−3</sup> and 10<sup>−4</sup> s<sup>−1</sup>, indicating that the forward reactions are competent. The actual reaction rates are certain to be larger



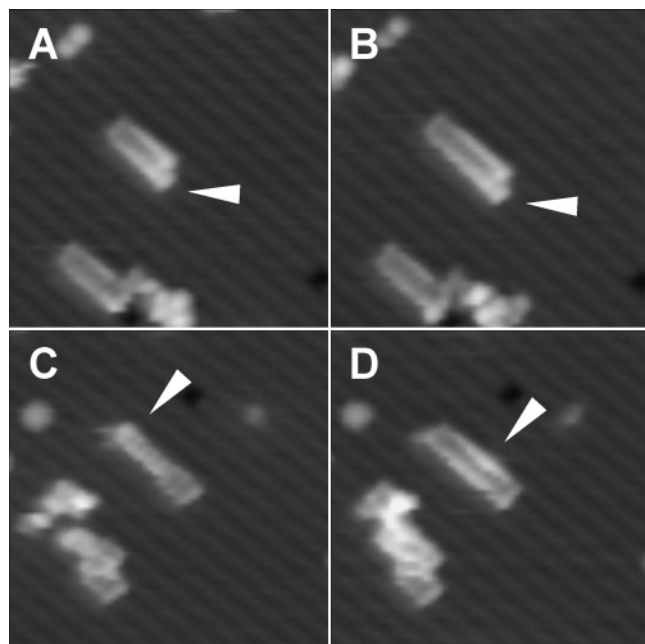


**Figure 4.** STM images demonstrating the mechanisms for aldehyde line growth. (A) Benzaldehyde double line that has a dangling bond at its end extends its growth (B) via the square wave mechanism upon additional exposure to benzaldehyde. (C) Nanostructure composed of double and single line portions with a dangling bond at the end of the single line. Further exposure to benzaldehyde leads to the formation of a complete double line through the antiparallel growth mechanism (D). Wedges indicate the location of the dangling bonds. STM images:  $12 \times 12$  nm,  $-3.5$  V,  $0.1$  nA.

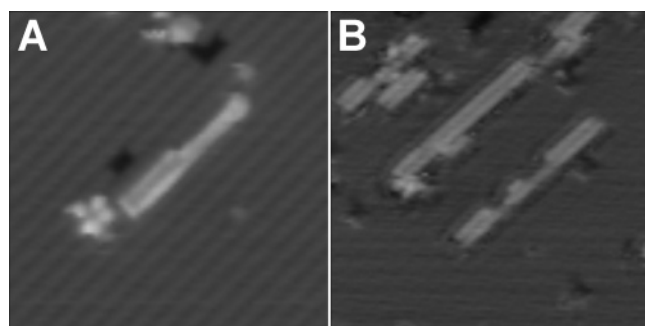


**Figure 5.** Mixed phases of single and double lines. (A) Nanostructure composed of single line and a double line segment. STM image:  $14 \times 14$  nm,  $-3.5$  V,  $0.1$  nA. (B) Nanostructure that has switched between single line and double line growth several times. STM image:  $20 \times 20$  nm,  $2.2$  V,  $0.5$  nA.

**TABLE 1: Reaction Energies and Barrier Heights Associated with the Line Growth of Aldehydes<sup>a</sup>**

reaction step	R = C <sub>6</sub> H <sub>5</sub>	R = CH <sub>3</sub>
addition (A $\rightarrow$ C)	-1.4	-1.1
abstraction barrier, next dimer (C $\rightarrow$ D)	1.0	0.7
H atom transfer, next dimer (C $\rightarrow$ E)	0.0	-0.5
total reaction, next dimer (A $\rightarrow$ E)	-1.4	-1.6
abstraction barrier, same dimer (C $\rightarrow$ F)	0.9	0.7
H atom transfer, same dimer (C $\rightarrow$ G)	0.0	-0.6
total reaction, same dimer (A $\rightarrow$ G)	-1.4	-1.6

<sup>a</sup> Values include zero-point energy corrections. The reaction steps are illustrated in Figure 2. All energies are in electron Volts.

than these values due to quantum mechanical tunneling, an effect that is known to play an important role in intramolecular H-atom transfer.<sup>25</sup>

In previous work, we showed that lower molecular weight alkenes were unable to grow lines.<sup>1</sup> Calculations revealed that

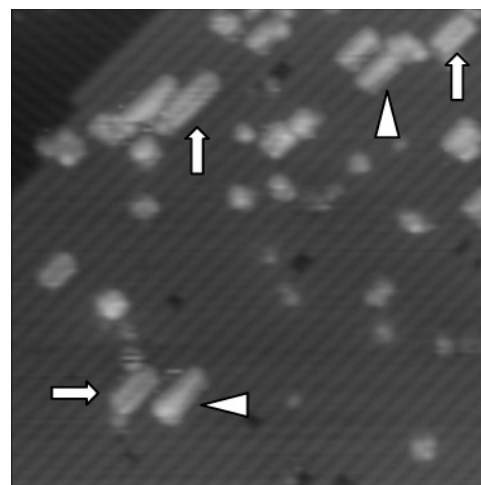


**Figure 6.** Acetaldehyde grows lines after great exposure of the surface to 120 Langmuirs. Short segments of both double (arrows) and single lines (wedges) are found. STM image:  $25 \times 25$  nm,  $-3.0$  V,  $0.065$  nA.

small, linear alkene molecules chemisorb to the surface, forming carbon-silicon  $\sigma$ -bonds of moderate strength. Molecules such as propylene might add to the surface but cannot easily grow lines because the critical, subsequent hydrogen atom abstraction step has an energy barrier that is substantially higher than its addition energy. The small molecules will therefore undergo desorption more readily than abstraction. The low molecular weight of propylene results in it having a short residence time on the surface and thus the molecule has a small number of addition attempts before going off into vacuum.

Aldehydes, on the other hand, can form strong silicon-oxygen  $\sigma$ -bonds, suggesting that low molecular weight species might grow lines on silicon. Our calculations (Table 1) support this suggestion: Acetaldehyde adds to the silicon dangling bond, releasing 1.1 eV. This chemisorption energy is less than that of benzaldehyde since the addition product associated with the latter benefits from the delocalization of the resulting carbon-centered, unpaired electron onto the phenyl ring.<sup>23</sup> The barriers to hydrogen atom abstraction by the added acetaldehyde from silicon atoms on the same dimer or on the next dimer in the row are essentially the same (0.7 eV) and are lower than the addition energy, implying that growth readily occurs. The overall exoergicity of the addition/abstraction process (A  $\rightarrow$  E or A  $\rightarrow$  G) is ca. 1.6 eV. The barrier to hydrogen atom abstraction in the case of acetaldehyde is ca. 0.3 eV lower than that for benzaldehyde, which suggests that line growth of the smaller molecule could occur. However, because acetaldehyde is only weakly physisorbed (due to its low molecular weight), we expect the line growth reaction to be difficult. We performed additional STM-UHV experiments wherein we exposed a silicon surface to acetaldehyde. Figure 6 shows that acetaldehyde does indeed undergo line growth reactions. As is the case for benzaldehyde, the lower molecular weight acetaldehyde grows double lines, but higher doses (viz., 120 L versus 5 L for benzaldehyde) are required to achieve reaction, which confirms our suspicions. The low physisorption energy of acetaldehyde means that these molecules have shorter surface residence times and reduces the likelihood of addition. We have previously demonstrated the role of physisorption in the self-directed line growth process.<sup>8</sup> In that work, it was observed that relatively large 1-undecene exhibited line growth while propylene did not.

One last feature observed in the STM images warrants comment: In Figure 4, the molecular lines appear bright near the DB, whereas molecules farther from the DB appear less

bright. We recently reported<sup>26</sup> that this “slope effect” is due to the Stark shifting of molecular orbitals by the DB, which is charged at the silicon crystal dopant level used in the present experiments.

### Concluding Remarks

We have studied the processes relevant to the formation of linear nanostructures of benzaldehyde and acetaldehyde on the hydrogen-terminated silicon(100) surface. STM experiments and quantum mechanical calculations indicate that different growth patterns for the lines are possible because of the essentially identical energetics and barrier heights associated with the different mechanisms for line growth. Understanding the growth of these molecules is particularly important because dialdehydes have the potential to undergo post-line-growth chemical modification, which will be explored in future work.

**Acknowledgment.** We thank Peter Kruse for performing some of the initial exploratory experiments. We thank the Centre for Excellence in Integrated Nanotools (University of Alberta) and WestGrid for access to computational facilities and iCORE, CIAR, and NSERC for financial support.

### References and Notes

- (1) Lopinski, G. P.; Wayner, D. D. M.; Wolkow, R. A. *Nature* **2000**, *406*, 48–51.
- (2) The naming convention we have used in the past to describe the composition of the nanostructures was based on polymer nomenclature, despite the fact that the nanostructures are not polymeric in nature. In this work, we have described linear nanostructures derived from benzaldehyde as “benzaldehyde lines”; however, the line growth process results in the reduction of the aldehyde moiety, giving lines of phenylcarbinolyl covalently bonded to the silicon surface.
- (3) Kruse, P.; Johnson, E. R.; DiLabio, G. A.; Wolkow, R. A. *Nano Lett.* **2002**, *2*, 807–810.
- (4) Pitters, J. L.; Piva, P. G.; Tong, X.; Wolkow, R. A. *Nano Lett.* **2003**, *3*, 1431–1435.
- (5) Pitters, J. L.; Wolkow, R. A. *J. Am. Chem. Soc.* **2005**, *127*, 48–49.
- (6) Tong, X.; DiLabio, G. A.; Wolkow, R. A. *Nano Lett.* **2004**, *4*, 979–983.
- (7) Tong, X.; DiLabio, G. A.; Clarkin, O. J.; Wolkow, R. A. *Nano Lett.* **2004**, *4*, 357–360.
- (8) DiLabio, G. A.; Piva, P. G.; Kruse, P.; Wolkow, R. A. *J. Am. Chem. Soc.* **2004**, *126*, 16048–16050.
- (9) Effenberger, F.; Gotz, G.; Bidlingmaier, B.; Wezstein, M. *Angew. Chem., Int. Ed.* **1998**, *37*, 2462–2464.
- (10) Boukherroub, R.; Morin, S.; Sharpe, P.; Wayner, D. D. M.; Allongue, P. *Langmuir* **2000**, *16*, 7429–7434.
- (11) Frisch, M. J.; Trucks, G. W.; Schlegel, H. B.; Scuseria, G. E.; Robb, M. A.; Cheeseman, J. R.; Montgomery, J. A., Jr.; Vreven, T.; Kudin, K. N.; Burant, J. C.; Millam, J. M.; Iyengar, S. S.; Tomasi, J.; Barone, V.; Mennucci, B.; Cossi, M.; Scalmani, G.; Rega, N.; Petersson, G. A.; Nakatsuji, H.; Hada, M.; Ehara, M.; Toyota, K.; Fukuda, R.; Hasegawa, J.; Ishida, M.; Nakajima, T.; Honda, Y.; Kitao, O.; Nakai, H.; Klene, M.; Li, X.; Knox, J. E.; Hratchian, H. P.; Cross, J. B.; Bakken, V.; Adamo, C.; Jaramillo, J.; Gomperts, R.; Stratmann, R. E.; Yazyev, O.; Austin, A. J.; Cammi, R.; Pomelli, C.; Ochterski, J. W.; Ayala, P. Y.; Morokuma, K.; Voth, G. A.; Salvador, P.; Dannenberg, J. J.; Zakrzewski, V. G.; Dapprich, S.; Daniels, A. D.; Strain, M. C.; Farkas, O.; Malick, D. K.; Rabuck, A. D.; Raghavachari, K.; Foresman, J. B.; Ortiz, J. V.; Cui, Q.; Baboul, A. G.; Clifford, S.; Cioslowski, J.; Stefanov, B. B.; Liu, G.; Liashenko, A.; Piskorz, P.; Komaromi, I.; Martin, R. L.; Fox, D. J.; Keith, T.; Al-Laham, M. A.; Peng, C. Y.; Nanayakkara, A.; Challacombe, M.; Gill, P. M. W.; Johnson, B.; Chen, W.; Wong, M. W.; Gonzalez, C.; Pople, J. A. *Gaussian 03*, revision C.02; Gaussian, Inc.: Wallingford, CT, 2004.
- (12) Becke, A. D. *J. Chem. Phys.* **1993**, *98*, 5648–5652.
- (13) Perdew, J. P. *Phys. Rev. B* **1986**, *33*, 8822–8824.
- (14) Johnson, E. R.; Clarkin, O. J.; DiLabio, G. A. *J. Phys. Chem. A* **2003**, *107*, 9953–9963.
- (15) The following reduced models were used in order to make the calculations feasible. For the addition reactions:  $\text{H}_2\text{CO} + \text{*Si}(\text{SiH}_3)_3$ . For the H-atom transfer reactions:  $\text{H}_2\text{CO}-\text{SiH}_2-\text{SiH}_2-\text{Si}^*(\text{SiH}_3)_2$ . The hydrogen atoms used to cap the silicon atoms in the model system were given Si–H bond lengths of 1.50 Å or C–H bond lengths of 1.11 Å.
- (16) Curtiss, L. A.; Redfern, P. C.; Raghavachari, K.; Rassolov, V.; Pople, J. A. *J. Chem. Phys.* **1999**, *110*, 4703–4709.
- (17) See for example: Svensson, M.; Humbel, S.; Froese, R. D. J.; Matsubara, T.; Sieber, S.; Morokuma, K. *J. Phys. Chem.* **1996**, *100*, 19357–19363.
- (18) Kang, K. J.; Musgrave, C. B. *J. Chem. Phys.* **2002**, *116*, 9907–9913.
- (19) (a) Hofer, W. A.; Fisher, A. J.; Lopinski, G. P.; Wolkow, R. A. *Chem. Phys. Lett.* **2002**, *365*, 129–134. (b) Cho, J.-H.; Oh, D.-H.; Kleinman, L. *Phys. Rev. B* **2002**, *65*, 081310.
- (20) Lee, J.-Y.; Cho, J.-H. *J. Chem. Phys.* **2004**, *121*, 8010–8013.
- (21) Takeuchi, N.; Selloni, A. *J. Phys. Chem. B* **2005**, *109*, 11967–11972.
- (22) The addition of triethylsilyl radical to benzaldehyde in solution has an activation energy of 0.14 eV. See Chatgililoglu, G.; Ingold, K. U.; Scaiano, J. C. *J. Am. Chem. Soc.* **1982**, *104*, 5119–5123.
- (23) DiLabio, G. A.; Litwinieko, G.; Lin, S.; Pratt, D. A.; Ingold, K. U. *J. Phys. Chem. A* **2002**, *106*, 11719–11725 and references therein.
- (24) The methods used to perform the calculations involve a number of approximations.<sup>15</sup> Thus, the computational approaches used likely cannot resolve energy differences < 0.1 eV.
- (25) Brunton, G.; Gray, J. A.; Griller, D.; Barclay, L. R. C.; Ingold, K. U. *J. Am. Chem. Soc.* **1978**, *100*, 4197–4200.
- (26) Piva, P. G.; DiLabio, G. A.; Pitters, J. L.; Zikovsky, J.; Rezek, M.; Dogel, S.; Hofer, W. A.; Wolkow, R. A. *Nature* **2005**, *435*, 658–661.